

Three-wave mixing with high amplification in a photorefractive polymer

A. Apolinar Iribe

*Departamento de Física, Universidad de Sonora (UNISON),
Apartado Postal. 1621, C.P.83000, Hermosillo, Sonora, México*

R.F. Domínguez Cruz

*Instituto Nacional de Astrofísica, Óptica y Electrónica (INAOE),
Apartado Postal 51 y 216, CP. 72000, Sta. Maria Tonantzintla, Puebla, México*

Recibido el 10 de diciembre de 2002; aceptado el 4 de junio de 2003

We demonstrate that in photorefractive polymer by crossing a strong and a weak beams one can achieve high intensity gains when the angle between them is small. The amplification of the weak wave is accompanied by the formation of the third beam produced by the strong beam diffraction into the -1 order. The gain obtained by the mechanism of three-wave mixing are much higher than the gains produced by earlier reported mechanisms. The experimental results are agree with the theoretical results obtained with the earlier for photorefractive crystals.

Keywords: Photorefractive polymers; photorefractive effect; nonlinear optics.

Demostramos que en un polímero fotorrefractivo en el cual se intersectan un haz fuerte y uno débil se obtienen altas ganancias cuando el ángulo entre los haces es pequeño. La amplificación del haz débil es acompañada por la formación de un tercer haz, el cual es producido por la difracción del haz fuerte en el orden -1 de difracción. La ganancia obtenida por el mecanismo de mezcla de tres ondas es mucho más alta que la producida por mecanismos reportados anteriormente. Los resultados experimentales concuerdan con los resultados teóricos obtenidos inicialmente para cristales fotorrefractivos.

Descriptores: Polímeros fotorrefractivos; efecto fotorrefractivo; óptica no lineal.

PACS: 42.70.Ln; 42.65.Hw; 82.35.Ej

1. Introduction

The progress in the field of molecular engineering has led to the development of a new generation of photorefractive materials that are organic [1]. The field of organic photorefractive materials was initiated in 1990 with the first evidence of the photorefractive effect in an organic crystal [2] and has grown rapidly after the demonstration of photorefractivity in a polymeric system [3-5]. Since the first proof of principle of photorefractivity in a polymer, the progress achieved in this new class of materials has been tremendous. In part, the rapid growth of the field can be attributed to technological promise and interesting physical properties of this material [6-8]. In addition to their compositional flexibility, photorefractive polymers benefit from low cost and ease of synthesis and processability. However, the most attractive feature is the large, fully reversible refractive index modulations ($\Delta n \sim 10^{-2}$) that can be achieved in these materials by light in real time by the PR effect [9]. On the other hand, one of the main limitations of PR polymers to date has been their need of very large applied electric fields. In practice, this has meant that materials rarely exceed a thickness of about $150 \mu\text{m}$, which in turn limits the achievable gain, $\gamma = \exp(\Gamma L)$, where L is the interaction length and Γ is the gain coefficient per unit length under optimum coupling conditions. For ΓL values commonly available, the net multiplicative gain factors would be in the range 2-5 [10].

The photorefractive effect is commonly described by the standard model of photorefractivity developed by Kukhtarev *et al.* [11]. For this model the mechanism of pho-

totrefractive gain, which involves two-wave mixing, the amplification occurs only if a phase shift of $\pi v y$ exists between the refractive index grating and interference fringes formed by the interacting beams [11]. In this situation the mechanism of charge transport is due to diffusion; otherwise, this depends on the relative intensity of the diffusion and drift processes. In general, the maximum space-charge field depends on the density of traps and the dielectric constant at low frequency. High doping levels are difficult to achieve in inorganic crystals, because they have the tendency to be repellent to the impurities. In polymers, the traps are not due to impurities but to structural defects or conformational disorders characteristic of the non crystalline material. As a result, very high density of traps can be present and the space-charge field can reach its saturation, because space charge field depends on the saturation field, which is proportional to the traps density, and the phase shift can be realized in steady-state as a result of trap saturation [12]. For small angles between beams, this mechanism does not work, and optimal fringe spacing is of an order of $1 \mu\text{m}$.

Alternative amplification mechanism involves three-wave non-Bragg interaction. It is closely related to modulational instability [13] and was demonstrated for non photorefractive materials [14-16] and, recently in PR ferroelectric SBN where 25 cm^{-1} gain was reported [17]. The distinctive feature of the mechanism is the formation of additional non-Bragg -1 st order in a process of two-wave mixing with a small angle between them: A weak signal beam and strong pump beam write a grating. A third beam is created by non-Bragg diffraction of the pump beam from the written grat-

ing. Interaction of these three beams yields amplification of the weak signal beam. The theory is discussed in detail in Ref. 18.

In this article, we report the results obtained for higher gain, than the gain produced by earlier reported mechanisms. We explain the dependencies using the three-wave mixing theory developed for PR crystals without saturation of trap centers.

2. Experimental setup

The composition of the PR polymer was NPAD-VBB:PVK:ECZ:TNF in the proportion 39:39:20:2 %wt. The polymer was based on the photoconductor poly-(N-vinylcarbazole) (PVK). The polymer composite contains 4-[(4'-nitrophenyl)azo]-1,3-bis[(3''-or 4''-vinylbenzyl)oxy]benzene (NPADVBB) as the nonlinear chromophore. A small amount of 2,4,7-trinito-9-fluorenone (TNF), which forms a charge-transfer complex with PVK, provided photosensitivity to visible light, and N-ethylcarbazole (ECZ) was added to lower the glass transition temperature. It is known, that to low concentrations of TNF, the charge transport is carried out mainly due to holes, while for high concentrations of TNF the transport of electrons is the predominant one. In photorefractive materials the same conduction of holes and electrons are not desired due to the migration of each species of carriers in the opposite direction which leads to a cancellation of the space charge. Therefore, the concentration of TNF in PVK has to be small ($< 2\%$) such that the conduction is mainly due to holes. The sample thickness is $105 \mu\text{m}$, it is placed between two transparent indium-tin-oxide (ITO) electrodes for application of an external electric field. The refractive index is 1.71 for 633 nm light.

The three-wave mixing was investigated in the typical tilted configuration (Fig. 1) with an external DC electric field. For a large photorefractive effect to be observed, the projection of the grating wave vector K on the applied electric field E should be large and the effective electrooptic coefficient is nonzero. At the same time, charge generation and transport are enhanced and the space charge field grows, giving rise to the photorefractive grating. For this, the tilt angle Ψ , defined by the sample normal and bisector between the write beams, was 60° in air. In order to generate a sinusoidal interference pattern in the PR polymer device, two linearly polarized beams derived from a He-Ne laser (633 nm, 10 mW) overlapped in the material. One strong beam and one weak beam have been crossed with small angle between them, $2\Theta_0$ (~ 0.065 rad.) Typical intensity ratio was 100:1. An external voltage was applied to the sample (the sign convention for the external field is explained in the Fig. 1).

3. Results and analysis

The additional -1st order appears as a result of grating formation when the external electric field is applied. The intensity

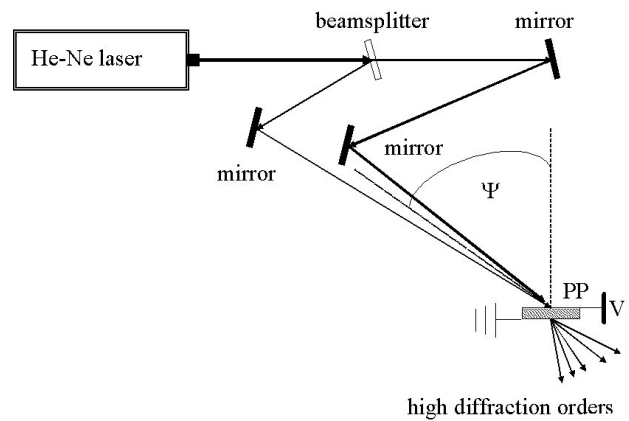


FIGURE 1. Geometry of three-wave mixing used in the photorefractive polymer. PP: photorefractive polymer and V: voltage.

of 3 diffraction orders after the polymer was measured by a photodetector. We observed up to nine diffraction orders.

Typical dependence of the 1st order intensity on the angle between beams is presented in the Fig. 2. Inverting the polarity of the electric field did not produce big changes in the curve. The difference is of the order of 5%.

For fitting the results we used Eqs. (3)-(4) of the Ref. 18. In this model only three beams and grating with a wave vector \mathbf{K} are taken into account. The intensity rapidly diminishes with the diffraction order, for our calculations we truncate the equations to take into account only the necessary number of these orders. It is assumed that the signal beam amplitude $S_1(z)$ and the additional beam amplitude $S_{-1}(z)$ are much smaller than the amplitude of the pump wave, which we take equal to one [$S_0(z)=1$], with zero absorption. The amplitude of the total electric field in the grating is represented in the following form:

$$E = \sum_{i=-1,0,1} S_i(z) \exp(-j\vec{\sigma}_i \cdot \vec{r}), \quad (1)$$

where $j = (-1)^{1/2}$, $\vec{r} = (x, y, z)$ and $\vec{\sigma}_i = \vec{\sigma}_0 - i\vec{K}$ with $\vec{\sigma}_0$ is the wavevector of the 0-th diffraction order in the medium, \vec{K} is the wave vector of the grating. $S_i(z)$ are amplitudes of corresponding diffraction orders. They are slowly varying along the direction of propagation, z .

We consider the case the stationary conditions, with no trap saturation and local response resulting from application of an external field. Then the refractive-index distribution along the x -axis is sinusoidal. It repeats the intensity distribution. The complex amplitude of grating is then

$$\Delta n(z) = (4\gamma/k_0) [S_{-1}^*(z) + S_1(z)], \quad (2)$$

with a real gain factor $\gamma = -k_0 n^3 r E^0 / 4$, where E^0 is the external electric field, k_0 is the wave number in free space, n_0 is the medium's refractive index and r is the effective electrooptic coefficient.

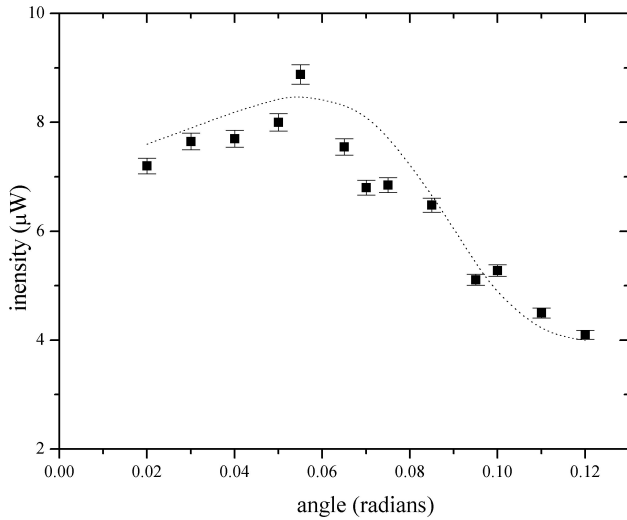


FIGURE 2. Weak beam intensity after the crystal vs. angle between beams for extraordinary polarization. The voltage -5 Kv is applied. Weak beam intensity after the crystal without external voltage is 4 μW; strong beam intensity is 420 μW. The dashed line is calculated using the truncated Eqs. (3)-(4).

If we suppose that the 0-th order remain undepleted [$S_0(z) = 1$] and by substituting Eqs. (1) and (2) into scalar wave (propagation of beams in a Keer medium [19])

$$i \frac{\partial E}{\partial z} + \frac{1}{2} \frac{\partial^2 E}{\partial x^2} + \kappa |E|^2 E = 0, \tag{3}$$

where κ is the nonlinear coefficient, which is positive for self-focusing media and negative for self-defocusing ones, we obtain the following system [18]:

$$\partial_z S_{-1} + j\vartheta_{-1} S_{-1} + 2j\gamma (S_{-1} + S_1^*) = 0, \tag{4}$$

$$\partial_z S_1 + 2j\gamma (S_1 + S_1^*) = 0. \tag{5}$$

The negative dephasing factor $\vartheta_{-1} = -K^2 / (k_0^2/n_0^2)$ depends on the angle between beams. To obtain Eqs. (4) and (5), we neglect the second derivatives $\partial_z^2 S_i(z)$. As small angles are involved we put the cosine of the Bragg angle equal to 1 and the amplitudes were normalized to the square root of the intensity of the central beam.

The general solution of Eqs. (4) and (5) is

$$S(z) = C_1 \exp(\lambda_1 z) + C_2 \exp(\lambda_2 z), \tag{6}$$

with

$$\lambda_{1,2} = \frac{1}{2} \left(j\vartheta_{-1} \pm \sqrt{-\vartheta_{-1}^2 - 8\gamma\vartheta_{-1}} \right), \tag{7}$$

and constants $C_{1,2}$ depending on the initial conditions. The growing exponential solution is possible if the expression under the square root is positive, *i.e.*, for γ positive (note that dephasing factors are negative), and $-\vartheta_{-1} < 8\gamma$. The maximal real part of λ is obtained for $\vartheta_{-1} = -4\gamma$ and it is equal to 2λ . For negative nonlinearity both roots are imaginary and no exponential gain exists. It follows from Eqs. (4)

and (5) that the intensity difference between 1st and -1st orders $S_1^* S_1 - S_{-1}^* S_{-1}$ remains constant with z for any γ , so the strong intensity growth of one beam will inevitably produce the growth in another one. For this case, if we initially have no -1st order, the 1st order will grow as

$$S_i(z) = S_i(0) \cosh(2\gamma z) \exp(-2j\gamma z). \tag{8}$$

Note that the exponential amplification is obtained only self-focusing nonlinearity ($\gamma > 0$).

The weak beam intensity after the crystal, as a function of angle between writing beams is show in the Fig. 2. The exact interpretation of this behavior is complicated by the fact that the gain is a convolution of the electro-optic response and the space charge field, which both depend in a complex fashion on the angle between the incident beams. It is seen that the amplification occurs for small angles. The angular dependence is well fitted by solution of Eqs. (4)-(5), with positive gamma. Assuming exponential gain [$\gamma = \exp(\Gamma L)$, where $z = L$ and $\gamma = -k_0 n^3 r E^0 / 4$], the intensity gain value is $\Gamma = \ln(8.88/4) / 0.01 = 80 \text{ cm}^{-1}$ for a voltage of 50V/μm. The maximal gain we were able to obtain for this voltage due to the traditional mechanism of trap saturation was 45 cm^{-1} [9]. Note, that according to the theory, the beam intensity inside the medium is given not by the $\exp(\gamma z)$, but rather by $\cosh(\gamma z)$, thus the apparent gain must be higher for thicker medium, with value approaching 4γ fitting $-\ln(4)$, *i.e.* about $50 \times 4 = 200 \text{ cm}^{-1}$.

The fitting values of Γ depending on voltage are presented in Fig. 3. It is seen that for higher voltages the gain grows as the square of the voltage. This dependence indicates that not only the electrooptic coefficient increases with the electric field but also the space-charge field. Because of limitations of the setup we were unable to raise the voltage above 5 kV, but voltages twice as high has been reported [12]. Raising the

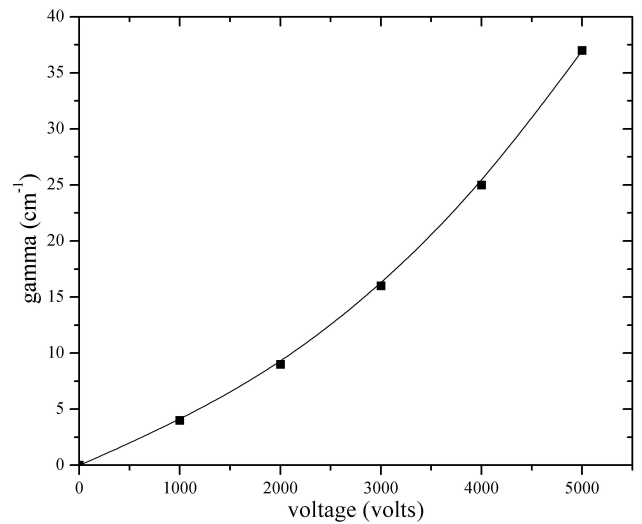


FIGURE 3. Amplification of the weak beam intensity versus voltage applied to the crystal for extraordinary polarization. The weak beam intensity after the crystal without external voltage is 4 μW; the strong beam intensity is 420 μW. The angle between weak and strong beams is 0.055 rad. The curve is guide for the eye.

voltage twice, one can expect the growth in gain-length product big enough to obtain noticeable noise amplification around the propagation direction similar to that one reported in SBN [17]. To obtain the generation observed in SBN, probably thicker samples are needed.

In conclusion, we have demonstrated that the three-wave mixing process of energy exchange is efficient in PR polymers. Its distinctive features are: small angle between beams, non-Bragg order participation, independence on voltage polarity, gains higher than traditional mechanism.

-
1. W.E. Moerner and S.M. Silence, *Chem. Rev.* **19** (1994) 127.
 2. J. Sutter, J. Hulliger, and P. Gunter, *Solid State Commun.* **74** (1990) 8678.
 3. K. Sutter and P. Gunter, *JOSA B* **7** (1990) 2274.
 4. S. Durcharme, J.C. Scott, R.J. Twieng, and W.E. Moerner, *Post-deadline paper OSA annual meeting* (Boston, 1990).
 5. S. Durcharme, J.C. Scott, R.J. Twieng, and W.E. Moerner, *Phys. Rev. Lett.* **66** (1991) 1846.
 6. L.A. Hornak, *Polymers for lightwave and Integrated Optics* (Marcel Dekker, New York, 1992).
 7. L.Y. Chiang, A.F. Garito, and D.J. Sandam (editors) *Matter. Res. Soc. Procc.* **247** (1992).
 8. J. Messier, F. Kajzar, and P.N. Prasad, *Organic Molecules for Nonlinear Optics and Photonics* (Kluwer Academic Press, Mass, 1991).
 9. K. Meerholz, B.L. Volodin, Sandalphon, B. Kippelen, and N. Peyghambarian, *Nature* **371** (1994) 497.
 10. A. Grunnet-Jepsen, C.L. Thompson, and W.E. Moerner, *Optics Commun.* **145** (1998) 145.
 11. N.V. Kukhtarev, V.B. Markov, S.G. Odulov, M.S. Soskin, and V.L. Vinestskii, *Ferroelectrics* **22** (1979) 949; *ibid.* **22** (1979) 961.
 12. A. Grunnet-Jepsen, C.L. Thompson, and W.E. Moerner, *JOSA B* **2** (1998) 905.
 13. V.I. Bespalov and V.I. Talanov, *JETP Lett.* **3** (1996) 307.
 14. A. Roy and K. Singh, *Phys. J. Appl. Phys.* **71** (1992) 5332.
 15. I.C. Khoo and T.H. Liu, *Phys. Rev. A* **39** (1989) 4036.
 16. I.C. Khoo, R. Normandin, T.H. Liu, R.R. Michael, and R.G. Lindquist, *Phys. Rev. B* **40** (1989) 7759.
 17. A. Apolinar-Irbe, N. Korneev, and J.J. Sánchez-Mondragón, *Optics Letters* **24** (1998) 1877.
 18. N. Korneev, A. Apolinar-Irbe, and J.J. Sánchez-Mondragón, *JOSA B* **4** (1999) 580.
 19. V.E. Zakharov and A.B. Shabat, *Sov. Physics JETP* **61** (1972) 62.